Lead-207 NMR Spectroscopy at 1.4 T:

Application of Benchtop Instrumentation to a Challenging *I* = ½ Nucleus

Short title: ^{207}Pb NMR Spectroscopy at 1.4 T

Guy M. Bernard and Vladimir K. Michaelis*

Gunning-Lemieux Chemistry Centre, 11227 Saskatchewan Drive, University of Alberta, Edmonton AB T6G 2G2 Canada

* Corresponding author: Vladimir K. Michaelis: Tel: 780-248-5893; Fax: 780-492-8231; email: vladimir.michaelis@ualberta.ca

Keywords: low-field NMR spectroscopy, permanent magnets, ^{207}Pb, solid-state NMR spectroscopy, solution NMR spectroscopy, lead nitrate, lead chloride, benchtop NMR spectroscopy

ABSTRACT

The practicality of obtaining liquid- and solid-state ^{207}Pb nuclear magnetic resonance (NMR) spectra with a low permanent-field magnet is investigated. Obtaining ^{207}Pb NMR spectra of salts in solution is shown to be viable for samples as dilute as 0.05 M. The concentration dependence of the ^{207}Pb chemical shifts for lead nitrate was investigated; the results are comparable to those obtained with high-field instruments. Likewise, the isotope effect of substituting D_2O for H_2O as the solvent was investigated and found to be comparable to those reported previously. Obtaining solid-state ^{207}Pb NMR spectra is challenging, but we demonstrate the ability to obtain such spectra for three unique solid samples. An axially symmetric ^{207}Pb powder pattern for lead nitrate and the powder pattern expected for lead chloride reveal linewidths dominated by shielding anisotropy, while ^{207}Pb-$^{35/37}$Cl *J*-coupling dominates in the methylammonium lead chloride perovskite material. Finally, recent innovations and the future potential of the instruments are considered.

INTRODUCTION

Since the introduction of NMR spectroscopy almost 75 years ago, the utility of the technique has driven continuous innovation, such as the introduction of superconducting NMR magnets, the application of Fourier transform techniques, pulse programming, the development of multiple-dimension techniques, and recently, the introduction of dynamic nuclear polarization (DNP) NMR spectroscopy,[1] which greatly enhances the sensitivity of the analytical method. Concurrent with these developments has been a trend towards higher magnetic fields with the goal of improving sensitivity and resolution.[2]

The benefits of higher magnetic fields are indisputable. Yet they also present several challenges for the NMR community, the most obvious of which is the expense of purchasing and maintaining a superconducting NMR magnet. Thus, there has recently been renewed interest in low-field permanent NMR magnets.[3] In addition to the much lower costs, benchtop instruments also offer the benefits of portability for field studies and are relatively compact, permitting their use in confined spaces such as fume hoods or glove boxes where real-time NMR monitoring of reactions becomes practical.[4] Acquisition of NMR spectra subject to very large anisotropic magnetic shielding or to chemical exchange may be impractical at high magnetic fields, either because of its excessive frequency range at high fields, or because this interaction induces unacceptably rapid relaxation.[5] Thus many research centres are finding low-field spectrometers to be a useful addition to their labs, either as a stand-alone instrument, or to complement data acquired with high-field instruments. NMR spectra can be acquired over a wide range of field strengths, from Earth's field, approximately 5×10^{-5} T (*i.e.*, a ^{1}H Larmor frequency of approximately 2 kHz),[6] to the highest currently available hybrid NMR magnets ($\mathbf{B}_0$ = 35.2 T, corresponding to a ^{1}H Larmor frequency of 1.5 GHz).[7] However, unless otherwise noted, in this report the discussion is

restricted to results obtained with a commercially available permanent low-field NMR magnet with a field strength of 1.4 T (*i.e.*, ^{1}H Larmor frequencies of approximately 60 MHz).

The ability to obtain ^{207}Pb NMR spectra at low magnetic field strengths was shown in the early days of NMR spectroscopy,[8] and studies on continuous wave (CW) instruments with a comparable magnetic field as those used in the present report were undertaken in the 1970s.[9] The first ^{207}Pb NMR measurements with a Fourier transform (FT) 2.1 T instrument were reported in 1973 by Maciel and Dallas.[10] However, despite being known since the early days of NMR spectroscopy,[11] such pulsed FT measurements did not become routine until commercial superconducting NMR magnets, available since 1964,[12] became the standard later in the decade. Thus, while NMR investigations have previously been conducted at field strengths currently available for benchtop instruments, the latter offer the benefits of pulsed FT NMR spectroscopy and the signal averaging potential inherent with that technique. Nevertheless, modern low-field instruments will not find much use unless one can obtain NMR spectra with signal to noise ratios that are comparable to those obtained with higher-field instruments.

Because compact permanent magnet spectrometers are a relatively recent innovation, the full scope of their potential has not been realized. In particular, research has generally been restricted to solution NMR studies of ^{1}H or other nuclei with high natural abundance (NA), such as ^{31}P (NA = 100 %) or to nuclei that have been isotopically enriched.[3] Thus, we asked ourselves two questions: i), is it practical to obtain NMR spectra of a relatively low-γ nucleus, ^{207}Pb (I = ½, NA = 22.1 %, Ξ = 20.920 %, ~20,000 ppm chemical shift range)? and ii), can one obtain ^{207}Pb NMR spectra of solid samples? We show that the answer to both questions is that it is indeed practical, though in some cases challenging, to undertake such studies due to various complications (*e.g.,*

sample, hardware, sensitivity, etc.) Finally, we consider possible extensions of the work presented here to other spin-½ nuclei or to quadrupolar nuclei with moderate quadrupolar coupling constants.

EXPERIMENTAL

Lead-207 NMR spectra were acquired at 1.4 T (^{1}H frequency = 60 MHz) on a commercially modified Nanalysis Corp. NMReady-60PRO^{TM} benchtop NMR spectrometer (Figure 1 (A)), operating at $\nu_L(^{207}\mathrm{Pb}) = 12.65$ MHz. The $\pi/2$ pulse widths were 14.9 μs ($\gamma B_1/2\pi$ = 17 kHz). For solution samples, recycle delays were 2.3 s and acquisition times were 1.5 s; recycle delays for solid samples were up to 15 s. All samples were placed in 5 mm solution NMR glass tubes. Solution samples were dissolved in either distilled H_2O or D_2O (99.9 % ^{2}H). The lock signal was obtained from either ^{2}H or ^{1}H of D_2O or H_2O, respectively; ^{207}Pb NMR spectra were indirectly referenced to tetramethyl lead (δ = 0 ppm) based on the ratio of the gyromagnetic frequencies of the lock signal nucleus of the solvent (^{2}H or ^{1}H) and that for ^{207}Pb. Thus, based on the frequency ratios reported by Harris *et al.*[13] and adjusting for the fact that the chemical shifts of H_2O or D_2O are assumed to be 4.78 ppm relative to the corresponding ^{1}H or ^{2}chemical shifts for TMS, the ^{207}Pb signal of tetramethyl lead was set to 20.920499 % that for ^{1}H of H_2O and 136.28449 % that for ^{2}H of D_2O. For solid samples, a powdered sample was placed at the bottom of a 5 mm glass NMR tube. A sealed capillary tube, filled with either H_2O or D_2O, was placed in the centre of the NMR tube (Figure 1 (B) and (C)) to provide the lock signal; if ^{1}H decoupling was not required, H_2O was the preferred source for the lock signal. The temperature of the sample was regulated at 305 K. Samples were not outgassed. Please note that, in some cases, this could impact the T_1 relaxation (and hence the line widths) and, in the case of averaged chemical shifts (*e.g.*, due to exchange) could impact the observed chemical shift. The ^{207}Pb T_1 relaxation time for a saturated $Pb(NO_3)_2$ sample dissolved in H_2O was determined using the progressive saturation technique.[14]

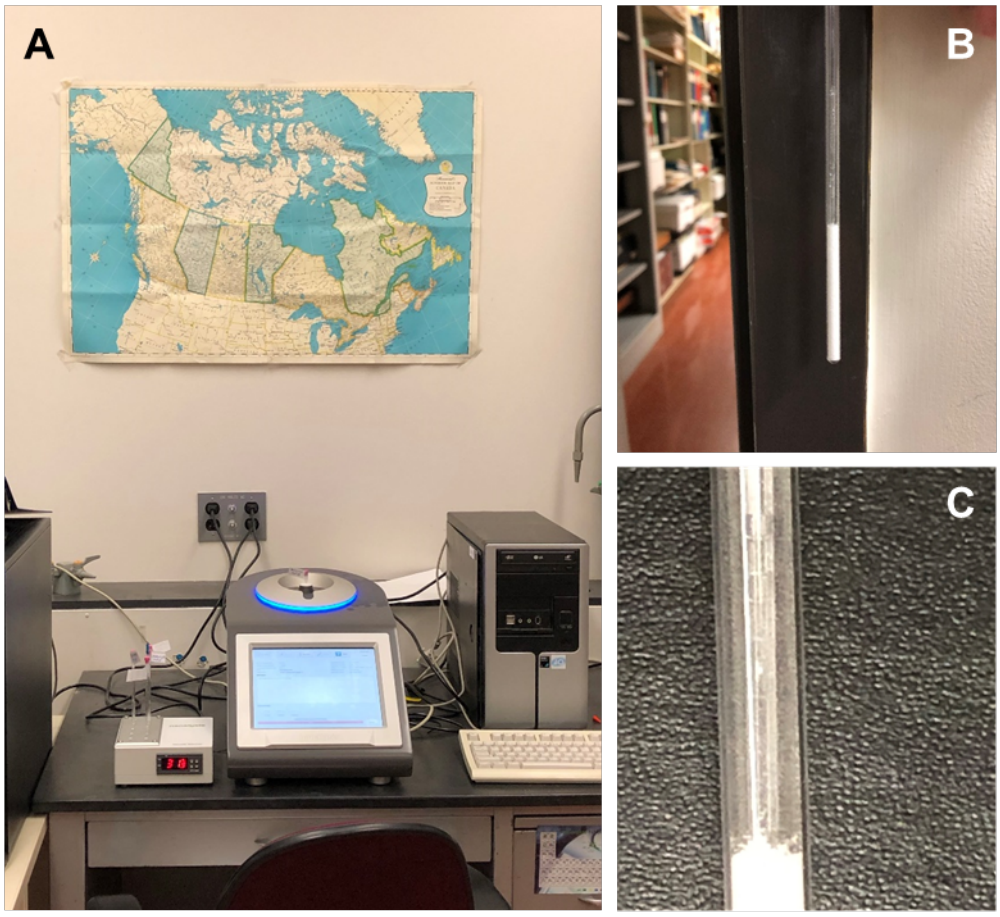

Figure 1. (A) An operating 1.4 T modified benchtop NMR spectrometer (weight - 25 kg; dimensions - 30 × 28 × 49 cm). The PC on the right, not part of the system, is included for perspective of instrument size. (B) A glass NMR tube with a capillary tube insert containing H_2O (for ^1H lock signal) and an expansion of the sealed capillary (C).

To measure the concentration dependence of the ^{207}Pb chemical shifts of lead nitrate dissolved in either H_2O or D_2O, a series of samples of various concentrations were prepared. Stock 1.0 M solutions were first prepared by transferring 8.31 g of the sample to a 25 ml volumetric flask. Approximately 2 ml of diluted samples, ranging from 0.05 to 0.8 M, were prepared by measuring with a digital pipette the appropriate volumes of stock solution and of either H_2O or D_2O that were then transferred to a vial and mixed.

^{1}H NMR spectra of a saturated solution of tetraphenyl lead dissolved in chloroform-*d* were acquired at 1.4 T on the Nanalysis system described above, operating at 60.45 MHz for ^{1}H. Spectra were acquired at 305 K using a 14.2 μs 90° excitation pulse. ^{1}H NMR spectra were also acquired at 9.4 T on an INOVA 400 NMR spectrometer operating at 300 K at 399.9 MHz for ^{1}H, using a 3.5 μs 30° excitation pulse.

Pb-207 NMR spectra of solid samples were also acquired on a Bruker NEO 500 11.75 T NMR spectrometer operating at 104.3 MHz for ^{207}Pb. Spectra were indirectly referenced to tetramethyl lead (δ = 0 ppm) based on the ^{1}H signal of methylammonium lead chloride following a procedure developed in this lab.[15] To compare data acquired with this instrument with those obtained at 1.4 T, the temperature was regulated at 305 K during data acquisition, using the BSVT temperature controller provided with the NEO 500. The temperature was calibrated based on the ^{207}Pb chemical shifts of methylammonium lead chloride as outlined in Reference [15]. Spectra were acquired with a Hahn echo pulse sequence, with π/2 and π pulses of 4.5 and 9.0 μs ($\gamma B_1/2\pi$ = 56 kHz), respectively, and with an interpulse delay of 23.25 μs; data were left-shifted post acquisition such that the FID began at the echo maximum. NMR spectra of solid samples were simulated using the WSolids software package.[16]

Solid-state NMR spectra are discussed according to the "Maryland Convention" proposed by Mason[17] and endorsed by IUPAC.[18] In this convention, three parameters are derived from the three principal components of the chemical shift tensor, δ_{11}, δ_{22} and δ_{33}:

$$\delta_{\mathrm{iso}} = {}^{1}\!/_{3}\,(\delta_{11} + \delta_{22} + \delta_{33}) \quad \textbf{(1)}$$

$$\Omega = (\delta_{11} - \delta_{33}) \quad \textbf{(2)}$$

$$\kappa = 3\frac{\delta_{22} - \delta_{\mathrm{iso}}}{\Omega} \quad \textbf{(3)}$$

RESULTS

Solution Samples

To initiate our investigation of low-field ^{207}Pb NMR spectroscopy, a spectrum of 1.0 M $Pb(NO_3)_2$ was acquired (Figure 2). Although data acquisition was permitted to continue through the night such that almost over 12,000 transients were co-added, it's notable that spectra obtained in less than two minutes (16 transients co-added; see inset to Figure 2) had sufficient signal-to-noise ratios for analyses such as calibrations (*e.g.*, pulse width and T_1 determination). The chemical shift, −2964 ppm, is close to the value of −2961 ppm reported by Maciel and Dallas[10] or by Harrison *et al*.[19] Prior to acquisition of the spectra illustrated in Fig. 2, the ^{207}Pb T_1 value for a saturated $Pb(NO_3)_2$ solution was determined to be 0.85(15) s, a small increase compared to the values of 0.491 and 0.487 s reported by Hays *et al*. for measurements obtained at 306 K at 2.35 and 7.05 T, respectively.[20] The T_1 relaxation times are related to the ^{207}Pb dynamics, such as Pb^{2+} interacting with the water molecules or ion pairing.[21] The small difference in values here preclude any definitive conclusions about these dynamics.

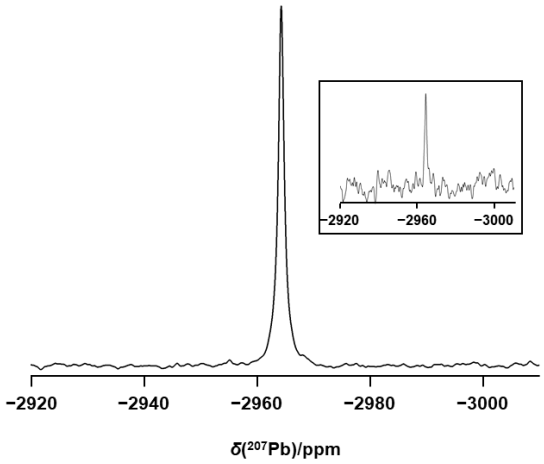

Figure 2. Lead-207 NMR spectrum of 1.0 M $Pb(NO_3)_2$ dissolved in H_2O, acquired at 1.4 T; 12,608 transients were co-added. The inset illustrates the spectrum for this sample obtained with only 16 co-added transients.

To assess the homogeneity of the induced field (γB_1) for the ^{207}Pb channel, a Bloch pulse calibration experiment for the commercial benchtop spectrometer was performed (Figure 3). Analyzing the initial 2π cycle provided a $\gamma B_1/2\pi$ of 14.9 kHz and a B_1 homogeneity of 0.46 was determined from the change in intensity between the 90° and 450° pulse width intensities (i.e., 450°/90°).[22] To further assess the B_1 homogeneity, a Fourier transform of the nutation curve was performed yielding a single resonance centred at 18 kHz and a full width at half maximum (fwhm) of 4 kHz. The pulse centre falls within the digital resolution of the Fourier transform and taking into consideration the width of the resultant peak. The frequency of the peak and its fwhm value represent the average RF field strength and the rate at which the induced field decay loses coherence, respectively, for the benchtop instrument operating at $\omega_L/2\pi$ of 12.6 MHz (^{207}Pb, $\mathbf{B_0}$ = 1.4 T). With these instrumental specifications we were able to record a good quality ^{207}Pb NMR spectrum of 1M $Pb(NO_3)_2$ in H_2O with a linewidth of 4 Hz (0.3 ppm) (Figure 2).

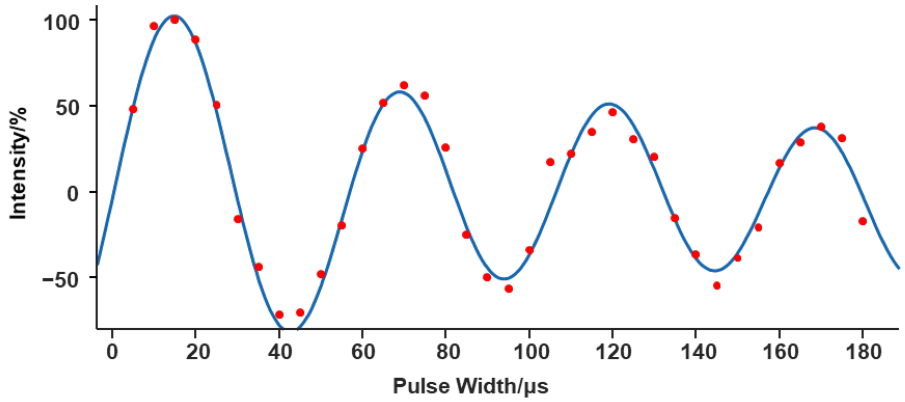

Figure 3. Lead-207 peak intensity as a function of excitation pulse width for 1.0 M $Pb(NO_3)_2$ dissolved in H_2O. Each point was acquired with 96 co-added transients. The blue line is the result of a fit to a damped sine function: $I = a1 \cdot \sin(b1x+c1) + a2 \cdot (\sin b2x+c2) + a3 \cdot (\sin(b3x+c3)$, where x is the pulse width and with $a1 = 244$, $b1 = 0.09$, $c1 = 1.47$, $a2 = 59.9$, $b2 = 0.12$, $c2 = -0.24$, $a3 = 234$, $b3 = 0.08$, $c3 = -1.47$; R^2 0.971, RMSE = 9.21.

The ^{207}Pb chemical shift is sensitive to the concentration of the sample;[19,23] this has been attributed to the rapid interchange of cations and anions in solution.[21,23] Such measurements may prove effective in an educational setting (vide infra) so we investigated whether the effect can be replicated at a lower field strength by acquiring spectra of a series of samples of various concentrations at 1.4 T. Figure 4A illustrates a plot of the chemical shifts of $Pb(NO_3)_2$ as a function of the concentration of this sample dissolved in H_2O. The observed trend is comparable to that reported by Harrison *et al.*[19] although at lower concentrations, our values suggest greater shielding, such that our predicted shielding at infinite dilution, −2885 ppm, is significantly greater than that predicted by Harrison and coworkers.[19] In contrast, Dybowski and coworkers[21] reported greater shielding values at lower concentrations than we observed. Previously, Lutz and Stricker reported a 72 ppm difference between the chemical shifts for 1.0 M $Pb(NO_3)_2$ and that expected for the sample at infinite dilution;[24] this compares to a range of 79 ppm observed here

and 108 ppm reported by Harrison *et al*.[19] Neue *et al*. have discussed factors, such as the temperature and concentration dependence of ^{207}Pb chemical shifts that explain many such discrepancies.[25]

Figure 4B illustrates the corresponding concentration dependence of $\delta(^{207}\text{Pb})$ as a function of concentration from $Pb(NO_3)_2$ dissolved in D_2O. The trend observed for this sample dissolved in H_2O is reproduced here, with the shielding increasing as a function of concentration. However, there are notable variations. For any given concentration, the shielding is greater for the sample dissolved in D_2O. For 1.0 M $Pb(NO_3)_2$ the solvent isotope shift, $\delta(^{207}\text{Pb},D_2O) - \delta(^{207}\text{Pb},H_2O) = -31$ ppm, is in agreement with the value reported in 1971 by Lutz and Stricker.[24] The effect increases with decreasing concentration, such that the difference increases to −51 ppm for the 0.05 M samples. The increasing solvent isotope shift with decreasing concentration is thought to be due to the fact that the equilibrium favours the formation of Pb^{2+} cations at lower concentrations, allowing for greater coordination with D_2O, while at higher concentrations, $Pb(NO_3)^+$ cations are favoured.[21]

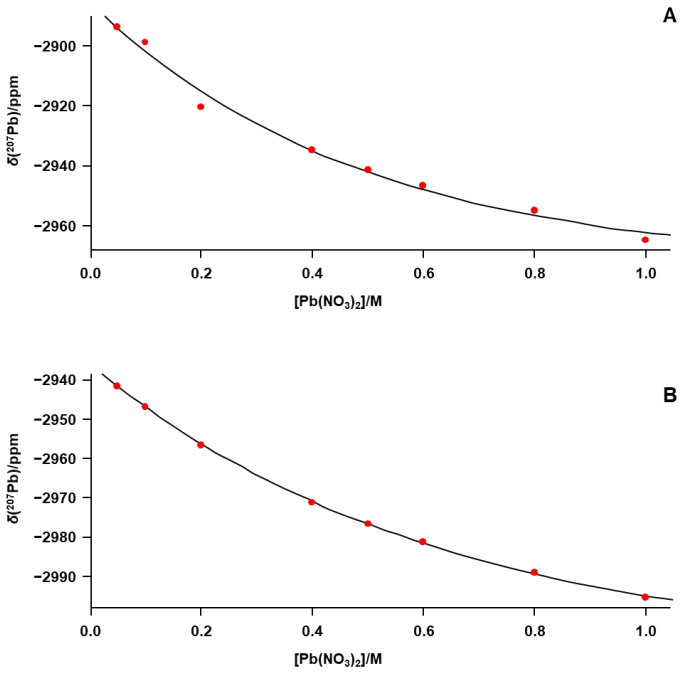

Figure 4. Plots of $\delta(^{207}Pb)$ vs concentration for $Pb(NO_3)_2$ dissolved in H_2O (A) or D_2O (B). The solid lines are fits assuming a 1st order exponential decay, with R^2 values of 0.9898 and 0.9996 for (A) and (B), respectively.

Solid Samples

Experimental and simulated ^{207}Pb NMR spectra of solid $Pb(NO_3)_2$ acquired at 1.4 T are illustrated in Figure 5A; for comparison, the corresponding spectra acquired at 11.75 T are shown in Figure 5B. Similar spectra[25,26] and those of MAS samples[27] have been reported previously; the sample has been of particular interest because of the sensitivity of the ^{207}Pb chemical shift to temperature.[28] Since the ^{207}Pb nucleus of $Pb(NO_3)_2$ is at a site of low crystal symmetry, its solid-state NMR spectrum is subject to anisotropic magnetic shielding.[29] From the reported crystal structure,[30] an axially symmetric chemical shift tensor is expected. This is apparent for the spectrum acquired at 11.75 T, but the expected powder pattern is also resolved for the spectrum

acquired at 1.4 T. The apparent lower resolution for that spectrum is a consequence of the fact that the spectra are displayed on the ppm scale (vide infra); in frequency units, the spectrum obtained at 1.4 T spans approximately 800 Hz while that acquired at 11.75 T spans 5.5 kHz. The chemical shift tensor of a given nucleus is a property of that nucleus and should be invariant to field, assuming the measurements are made under the same conditions (*e.g.*, temperature, phase, *etc*.) Table 1 summarizes the chemical shift tensor parameters obtained from simulations of the data; values are similar.

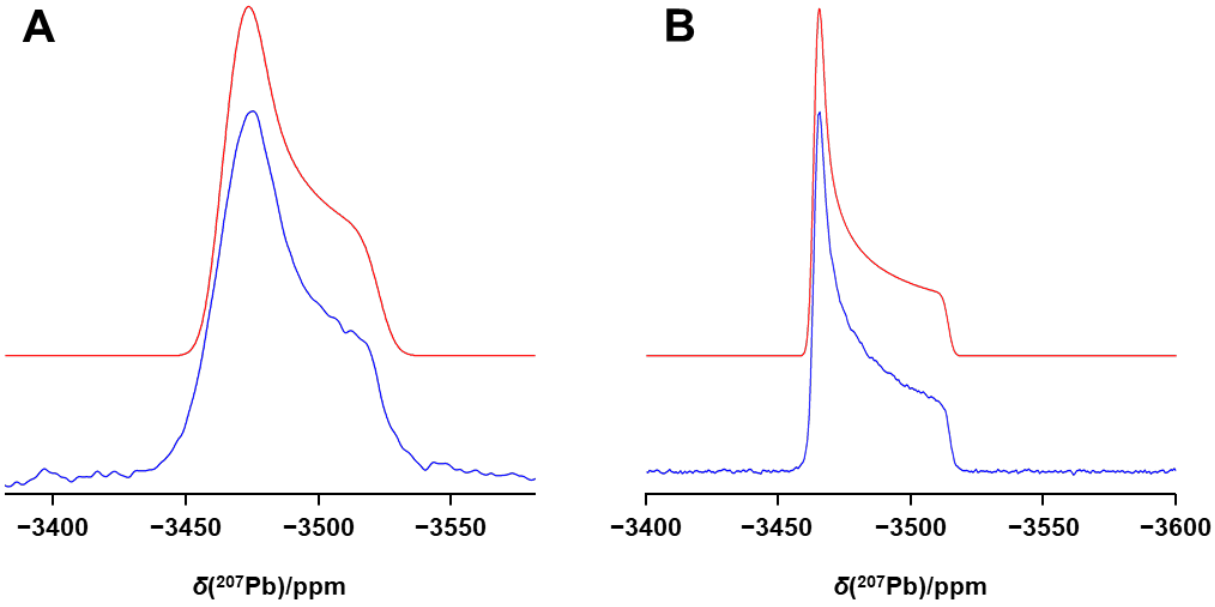

Figure 5. Simulated (upper red traces) and experimental (lower blue traces) ^{207}Pb NMR spectra of solid $Pb(NO_3)_2$, acquired at 1.4 T (A) and 11.75 T (B). Spectra were acquired at 305 K on nonspinning samples.

Table 1. Chemical shift tensor parameters for solid $Pb(NO_3)_2$ and $PbCl_2$.

	$Pb(NO_3)_2$		$PbCl_2$	
	1.4 T	11.75 T	1.4 T	4.7 T[a]
δ_{11}/ppm	−3470(8)	−3464(1)	−1492(12)	−1490
δ_{22}/ppm	−3470(4)	−3464(1)	−1686(8)	−1627
δ_{33}/ppm	−3525(3)	−3514(1)	−2057(10)	−2046
δ_{iso}/ppm	−3488(2)	−3481(1)	−1745(6)	−1721(2)
Ω/ppm	55(6)	50(1)	565(16)	556(4)
κ	1.0(4)	1.00(5)	0.3(1)	0.505(23)

a. Data were obtained in our lab at 305 K apart from those for $PbCl_2$ acquired at 4.7 T, which were obtained at room temperature by Dmitrenko *et al.* [31]

Figure 6A illustrates the ^{207}Pb NMR spectrum of $PbCl_2$ acquired at 1.4 T. The chemical shift, $\delta_{iso} = -1745 \pm 6$ ppm, is slightly lower than the value of -1721 ± 2 ppm reported by Dmitrenko *et al.*;[31] a similar value was reported by Dybowski *et al.*[32] Table 1 summarizes the chemical shift tensor principal components obtained by us and by Dmitrenko *et al.*[31] As for the ^{207}Pb spectra for $Pb(NO_3)_2$ discussed above, the distinct features arising from anisotropic magnetic shielding in $PbCl_2$ are not as clearly defined but still measurable at 1.4 T. Each ^{207}Pb nucleus in $PbCl_2$ is coordinated to nine ^{35}Cl or ^{37}Cl nuclei (both $I = 3/2$, with natural abundances of 75.78 and 24.22 %, respectively) with six distinct Pb-Cl bond lengths.[33] Thus, a given ^{207}Pb nucleus is susceptible to broadening due to dipolar and J spin-spin coupling from both ^{35}Cl and ^{37}Cl nuclei from a total of nine chlorine nuclei with six distinct environments; because these interactions are invariant to field strength, the apparent broadening, on the ppm scale, is greater at lower fields (see below).

The pattern is further complicated by effects of these quadrupolar nuclei on ^{207}Pb, which is greater at lower field strengths.[34] In addition, the combination of magnetic shielding anisotropy and spin-spin interactions resulted in a spectrum that covered a significant portion of the 1000 ppm chemical shift range of our 1.4 T instrument. For such spectra acquired with a moderately long 90° pulse, non-uniform excitation may also be a factor in the observed line shape. For spectra with broader powder patterns, the variable offset cumulative spectra (VOCS) technique[35] may be essential.

Figure 6B illustrates ^{207}Pb NMR spectra for methylammonium lead choride ($MAPbCl_3$) acquired at 1.4 and 11.75 T. Similar spin-spin interactions (as discussed above for $PbCl_2$) are a factor in the line shape, but because the ^{207}Pb nuclei in $MAPbCl_3$ are at a centre of cubic symmetry, magnetic shielding anisotropy is no longer a contributing factor in this case. Bernard *et al*. have presented a detailed discussion of how the spin-spin interactions impact the ^{207}Pb NMR line shape for this sample.[36] The slightly broader spectrum at 1.4 T is attributed to a breakdown of the high-field approximation[34] because the quadrupolar interactions for the $^{35/37}$Cl nuclei are a significant fraction of the ^{207}Pb Larmor frequency; the nuclear quadrupole frequency for ^{35}Cl of $MAPbCl_3$ is 8.1 MHz.[37]

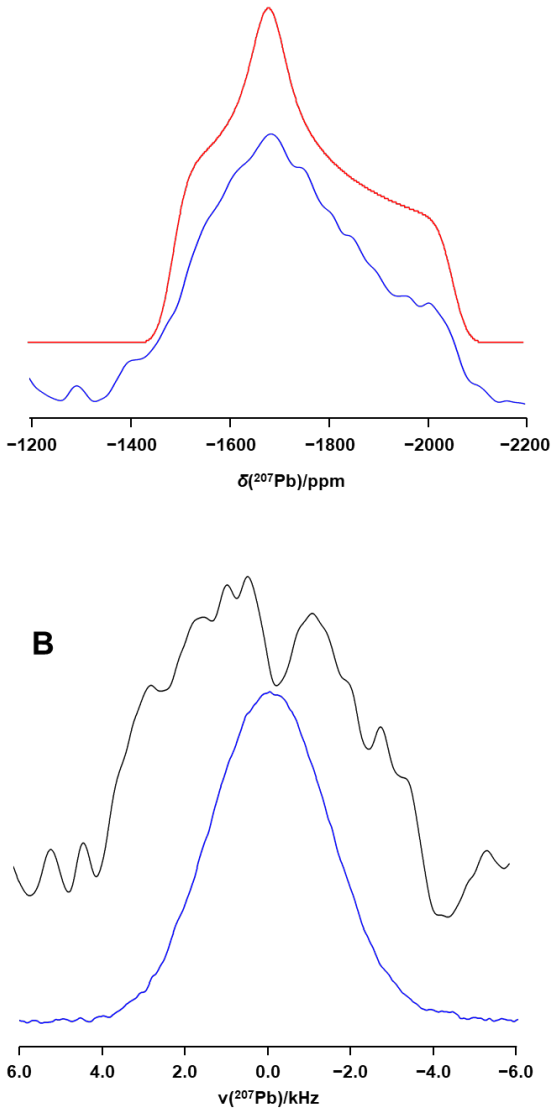

Figure 6. (A) Simulated (upper red trace) and experimental (lower blue trace) ^{207}Pb NMR spectra of a nonspinning sample of $PbCl_2$, acquired at 1.4 T at 305 K. (B) ^{207}Pb NMR spectra of a nonspinning sample of $MAPbCl_3$, acquired at 1.4 T (black trace) and at 11.75 T (blue trace). The spectrum acquired at 1.4 T is the sum of 73,576 transients and required in excess of 4 days to acquire. In contrast, the spectrum acquired at 11.75 T was obtained in less than one hour (760 transients). The centre of these two spectra were arbitrarily set to 0 kHz to allow comparison on the frequency scale of spectra acquired at different fields.

DISCUSSION

A general overview of the use of a relatively low-field permanent magnet for the acquisition of ^{207}Pb NMR spectra has been presented. Obtaining such spectra for samples in solution is straightforward and, unless one is trying to resolve a complex spin system, should yield spectra of acceptable quality for typical analyses, such as characterisation of samples often encountered in research or teaching laboratory settings. The success demonstrated here for ^{207}Pb is encouraging, not only for NMR studies of this nucleus, but also for studies of other less commonly observed nuclei. The receptivity of this nucleus relative to that for ^{1}H, 2.01×10^{-3},[18] is comparable to those for many other spin-½ nuclei. Thus, with the necessary hardware modifications, spin-½ nuclei such as $^{111/113}$Cd or ^{119}Sn may be accessible; a similar instrument has already been used to acquire ^{29}Si and ^{15}N NMR spectra. Of course, as for high-field instruments, isotopic enrichment usually renders NMR spectroscopy of more challenging nuclei practical. In addition, quadrupolar nuclei ($I > 1/2$) with small quadrupole moments and comparable receptivity such as ^{133}Cs may also be accessible. Indeed, NMR studies of quadrupolar nuclei (^{7}Li, ^{23}Na and ^{27}Al) have been undertaken as early as 1950,[38] at magnetic field strengths as low as 0.12 T. See reference [39] for an early review on the topic. The practicality of obtaining solution ^{7}Li NMR spectra with a benchtop instrument has been demonstrated;[40] this is an intriguing aspect considering the role NMR spectroscopy plays in the study of battery materials (e.g., Li-ion dynamics).

As is true for solid-state NMR spectroscopy using high-field superconducting magnets, obtaining spectra of solid samples with the permanent magnet considered in this study at times proved challenging. The relative receptivity considerations discussed above are a factor when extending the application of solid-state NMR spectroscopy to other nuclei, but other factors also come into play; for example, the anisotropic magnetic shielding that gives rise to the powder line

shapes observed for ^{207}Pb NMR spectra for $Pb(NO_3)_2$ and $PbCl_2$ (Figures 5 and 6) also impacts the sensitivity,[29] since the signal from a given nucleus extends over a much broader range than it does for the same sample in solution. The effect of the nuclear quadrupolar interaction on NMR spectra is inversely related to the magnetic field strength and thus impacts the practicality of obtaining solid-state NMR spectra of quadrupolar nuclei on low-field permanent magnets, unless the quadrupoalar nuclei are at a site of high symmetry and hence have a negligible nuclear quadrupolar interaction.[41] Thus, many quadrupolar nuclei may be accessible for solid-state NMR studies at low field regardless of quadrupole moment if the nucleus of interest is located in a highly symmetric site or when the quadrupole moment is very small. Further hardware advances, expected in the coming years, will surely drive the application of the technique to analyses of more complex spin systems (*vide infra*).

Fig. 7 illustrates both the strengths and weaknesses of applying benchtop NMR spectroscopy to a "real world" problem. The ^{1}H NMR spectrum shown here, of saturated tretraphenyl lead in chloroform, was acquired with and without ^{207}Pb decoupling at 1.4 and 9.4 T. At 1.4 T, the small chemical shift differences between the three distinct ^{1}H nuclei (ortho, meta and para to the carbon bonded to Pb) results in a crowded and complex second-order spin system;[42] the spin-spin coupling to ^{207}Pb further complicates the spectrum in the absence of decoupling of this nucleus. Note that, in frequency units, the fwhm for spectra acquired at both fields are comparable, but because the spectra in this figure are plotted on the ppm scale, those obtained at 1.4 T appear to be broader (*i.e.*, a fwhm of 6 Hz is 0.1 ppm at 1.4 T but the same value corresponds to less than 0.02 ppm at 9.4 T). Nevertheless, useful information is gained by comparing ^{1}H spectra obtained with and without ^{207}Pb decoupling at 1.4 T. For example, a synthetic chemist trying to confirm the synthesis of tetraphenyl lead would confirm that the high-frequency pair of peaks are a

consequence of $^{3}J(^{207}\text{Pb},^{1}\text{H})$, and that the sample consists of only aromatic sites, consistent with the target compound.

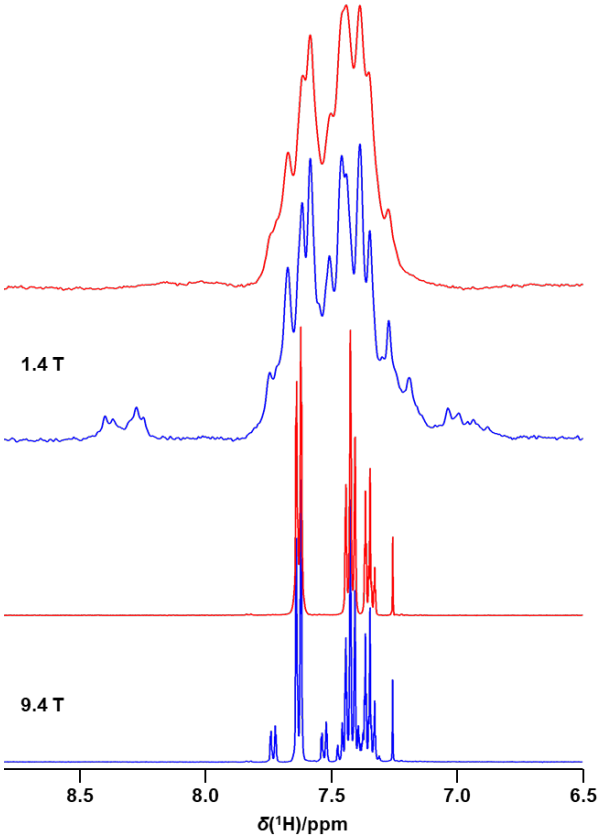

Figure 7. ^{1}H (blue traces) and ^{1}H{^{207}Pb} (red traces) NMR spectra of saturated tetraphenyl lead in chloroform-*d*, acquired at 1.4 T (upper traces) and at 9.4 T (lower traces).

PERSPECTIVES

Despite the challenges, the practicality of obtaining solid-state ^{207}Pb NMR spectra of solid samples has been demonstrated. Extension of the technique to "real world" problems is remarkably attractive in certain situations. It may also be practical to obtain qualitative or quantitative solution or solid-state ^{207}Pb NMR spectra of basic spin systems that answer questions of interest for commercial applications (*e.g.*, has the starting Pb-containing material fully reacted?

or, can we quantify the residual Pb^{2+} in solution?). Such labs often incur extensive fees for the acquisition of NMR spectra at off-site high-field NMR labs. At a minimum, preliminary spectra could be obtained with a benchtop instrument to decide whether the expenses and delays related with obtaining a high-field NMR spectrum are warranted. In addition, its small size renders it amenable for siting in enclosed spaces such as glove boxes, and it is ideal for field work.

Another area where the instrument has tremendous potential is in education. Of course, NMR spectroscopy is a key component of undergraduate training for chemistry students, and for those studying in related fields such as chemical engineering. Yet, financial constraints often preclude the acquisition of superconducting NMR spectrometers, especially for smaller institutions. Understandably, administrators are also reluctant to allow access to sensitive equipment by large groups of inexperienced students, particularly when proper supervision is difficult. Benchtop systems offer solutions to both these problems. In fact, some important NMR concepts, such as the effects on solution NMR spectra of tightly coupled spin systems, are more easily demonstrated with a low-field instrument. Other concepts (*e.g.*, T_1 measurements and the analysis of the resulting data) may be demonstrated as well with a benchtop instrument as with a superconducting NMR spectrometer, obviating the necessity of a high-field instrument for student education, or freeing it for research. Another example is the possibility of tracking exchange phenomena, as we demonstrated above for aqueous $Pb(NO_3)_2$. Undergraduate students are rarely exposed to solid-state NMR spectroscopy although the technique may be important in their future careers. Although it is improbable that laboratory coordinators will incorporate a ^{207}Pb NMR section into their undergraduate laboratory curriculum, we have demonstrated that chemical shift anisotropy is detectable at 1.4 T in ^{207}Pb NMR spectra $Pb(NO_3)_2$; a more innocuous nucleus (*e.g.*, ^{31}P) in a sample that yields similar spectra would be very educational. We note that some caution must be

exercised if one attempts ^{207}Pb NMR spectroscopy within undergraduate research settings. Locating the reference signal may be a challenge (20,000 ppm chemical shift range) as conventional acquisition parameters and probe bandwidths are limited. This could create some difficulties for the novice NMR user to locate a real signal. Finally, in addition to technical aspects of acquiring ^{207}Pb NMR spectra, one needs to identify the associated safety precautions necessary when handling lead-containing compounds, including safe handling, preparation and disposal procedures.

As for other forms of NMR spectroscopy, progress in the development of benchtop NMR spectroscopy has been continuous such that it is now readily available with a portable footprint smaller than a conventional microwave – truly desktop NMR spectroscopy! In a trend mimicking earlier developments in NMR magnets, higher-field benchtop magnets are being introduced. For example, Nanalysis Corp. recently introduced a 100 MHz benchtop NMR spectrometer,[43] and 80 MHz benchtop instruments have been introduced by Magritek Ltd.[44] and by Bruker Biospin.[45] With time, innovations that have greatly advanced high-field NMR spectroscopy will surely be applied to permanent benchtop magnets. For example, magic-angle spinning, which has greatly enhanced the resolution of solid-state NMR spectra, has recently been applied to low-field instruments.[46] Pulse programs, either modified from those used for high-field spectrometers or innovations specific to these instruments, as well as recent innovations (such as dynamic nuclear polarization),[1] will surely evolve to enhance the far-reaching capabilities of these instruments. As techniques continue to improve, the applicability of benchtop NMR spectroscopy in various endeavours will surely continue to grow!

CONCLUSIONS

Although challenges remain, benchtop NMR spectrometers will surely become part of the "toolkit" for many chemistry departments. As for many other new techniques, these systems are not an alternative to established techniques, but rather complement the information gained at high fields due the unique field dependencies of various NMR interactions. In the work presented herein, we demonstrated that obtaining solution and solid-state NMR spectra of the ^{207}Pb nucleus (and by extension, other nuclei with similar nuclear properties) is possible. One can foresee the day when benchtop NMR spectrometers take their place alongside other instruments as essential tools for researchers.

ACKNOWLEDGEMENTS

The authors are very grateful to Nanalysis Corp. for providing the NMReady-60PRO™ instrument used for the results reported herein, and to their staff for many helpful discussions, modifications and suggestions. We acknowledge the Natural Sciences and Engineering Research Council of Canada (NSERC) and the Government of Alberta (Campus Alberta Small Business Engagement program) for funding. We thank Prof. Roderick Wasylishen for scientific discussions. We also thank Mr. Mark Miskolzie for obtaining some high-field solution NMR spectra, as well as Ms. Mya Dodd, Ms. Michelle Ha and Mr. Diganta Sarkar for some preliminary results in relation to this project.

REFERENCES

[1] a) *Handbook of High Field Dynamic Nuclear Polarization* (Eds. V. K. Michaelis, R. G. Griffin, B. Corzilius, S. Vega), Wiley, Chichester, UK, **2020**. b) R. G. Griffin, T. M. Swager, R. J. Temkin, *J. Magn. Reson*. **2019**, *306*, 128; c) G. M. Bernard, V. K. Michaelis, *eMagRes*, **2019**, *8*, 77−86, DOI: 10.1002/9780470034590.emrstm1560; d) A. G. M. Rankin, J. Trébosc, F. Pourpoint, J.-P. Amoureux, O. Lafon, *Solid State Nucl. Magn. Reson*. **2019**, *101*, 116; e) M. Ha, V. K. Michaelis, in *Modern Magnetic Resonance* (Ed. G. Webb), Springer, Cham, Switzerland, **2017**, p. 1; f) V. K. Michaelis, T.-C. Ong, M. K. Kiesewetter, D. K. Frantz, J. J. Walish, E. Ravera, C. Luchinat, T. M. Swager, R. G. Griffin, *Isr. J. Chem*., **2014**, *54*, 207.

[2] R. Teodorescu, in *Modern NMR Approaches to the Structure Elucidation of Natural Products, Vol. 1: Instrumentation and Software* (Eds.: A. J. Williams, G. E. Martin, D. Rovnyak) Royal Society of Chemistry, London, **2016**, Chapter 2, pp. 26 – 37.

[3] a) M. Grootveld, B. Percival, M. Gibson, Y. Osman, M. Edgar, M. Molinari, M. L. Mather, F. Casanova, P. B. Wilson, *Anal. Chim. Acta*, **2019**, *1067*, 11; b) B. Blümich, *Trends Anal. Chem*. **2016**, *83*, 2; c) B. Blümich, S. Haber-Pohlmeier, W. Zia, *Compact NMR*, Walter de Gruyter, Berlin, **2014**.

[4] K. Singh, E. Danieli, B. Blümich, *Anal. Bioanal. Chem*. **2017**, *409*, 7223.

[5] S. F. Cousin, P. Kadeřávek, B. Haddou, C. Charlier, T. Marquardsen, J.-M. Tyburn, P.-A. Bovier, F. Engelke, W. Maas, G. Bodenhausen, P. Pelupessy, F. Ferrage, *Angew. Chem. Int. Ed*. **2016**, *55*, 9886; *Angew. Chem.* **2016**, *128*, 10040.

[6] M. E. Halse, P. T. Callaghan, in *Encyclopedia of NMR, Vol. 9* (Eds.: R. K. Harris, R. E. Wasylishen) Wiley, Chichester, **2012**, pp. 5060 – 5065.

[7] Z. Gan, I. Hung, X. Wang, J. Paulino, G. Wu, I. M. Litvak, P. L. Gor'kov, W. W. Brey, P. Lendi, J. L. Schiano, M. D. Bird, I. R. Dixon, J. Toth, G. S. Boebinger, T. A. Cross, *J. Magn. Reson*. **2017**, *284*, 125.

[8] See, for example, a) E. D. Baker, *J. Chem. Phys.* **1957**, *26*, 960, b) J. M. Rocard, M. Bloom, L. B. Robinson, *Can. J. Phys*. **1959**, *37*, 522.

[9] See, for example, a) W. G. Schneider, A. D. Buckingham, *Discuss. Faraday Soc.* **1962**, *34*, 147, b) H. Fuβstetter, H. Nöth, B. Wrackmeyer, W. McFarlane, *Chem. Ber.* **1977**, *110*, 3172.

[10] G. E. Maciel, J. L. Dallas, *J. Am. Chem. Soc*. **1973**, *95*, 3039.

[11] T. C. Farrar, *Anal. Chem.* **1970**, *42*, 109A.

[12] H. Maeda, Y. Yanagisawa, *J. Magn. Reson.* **2019**, *306*, 80.

[13] R. K. Harris, E. D. Becker, S. M. Cabral de Menezes, R. Goodfellow, P. Granger, *Pure Appl. Chem.* **2001**, *73*, 1795.

[14] R. Freeman, H. D. W. Hill, *J. Chem. Phys.* **1971**, *54*, 3367.

[15] G. M. Bernard, A. Goyal, M. Miskolzie, R. McKay, Q. Wu, R. E. Wasylishen, V. K. Michaelis, *J. Magn. Reson*. **2017**, *283*, 14.

[16] K. Eichele, WSolids NMR Simulation Package, V. 1.21.3, Universität Tübingen, 2015.

[17] J. Mason, *Solid State Nucl. Magn. Reson*. **1993**, *2*, 285.

[18] R. K. Harris, E. D. Becker, S. M. Cabral de Menezes, P. Granger, R. E. Hoffman, K. W. Zilm, *Pure Appl. Chem*. **2008**, *80*, 59.

[19] P. G. Harrison, M. A. Healy, A. T. Steel, *J. Chem. Soc. Dalton Trans*. **1983**, 1845.

[20] G. R. Hays, D. G. Gillies, L. P. Blaauw, A. D. H. Clague, *J. Magn. Reson*. **1981**, *45*, 102.

[21] N. Altounian, A. Glatfelter, S. Bai, C. Dybowski, *J. Phys. Chem. B*, **2000**, *104*, 4723.

[22] P. A. Keifer, *Conc. Magn. Reson*. **1999**, *11*, 165.

[23] a) F. Alkan, T. Small, S. Bai, A. Dominowski, C. Dybowski, *J. Struct. Chem*. **2016**, *57*, 369; *Zhurn. Strukt. Khim.* **2016**, *57*, 382; b) A. M. de P. Nicholas, R. E. Wasylishen, *Can. J. Chem.* **1987**, *65*, 951.

[24] O. Lutz, G. Stricker, *Phys. Lett.* **1971**, *35A*, 397.

[25] G. Neue, C. Dybowski, M. L. Smith, M. A. Hepp, D. L. Perry, *Solid State Nucl. Magn. Reson*. **1996**, *6*, 241.

[26] P. J. de Castro, C. A. Maher, R. L. Vold, G. L. Hoatson, *J. Chem. Phys*. **2008**, *128*, 052310.

[27] a) Y.-S. Kye, B. Herreros, G. S. Harbison, *J. Phys. Chem. B*, **2001**, *105*, 5892; b) Y.-S. Kye, G. S. Harbison, *Inorg. Chem*. **1998**, *37*¸ 6030.

[28] a) M. Kitamura, A. Asano, *Anal. Sci*. **2013**, *29*, 1089; b) X. Guan, R. E. Stark, *Solid State Nucl. Magn. Reson*. **2010**, *38*, 74; c) J.-B. d'Espinose de Lacaillerie, B. Jarry, O. Pascui, D. Reichert, *Solid State Nucl. Magn. Reson*. **2005**, *28*, 225; d) P. A. Beckmann, C. Dybowski, *J. Magn. Reson*. **2000**, *146*, 379; e) L. C. M. van Gorkom, J. M. Hook, M. B. Logan, J. V. Hanna, R. E. Wasylishen, *Magn. Reson. Chem.* **1995**, *33*, 791; f) A. Bielecki, D. P. Burum, *J. Magn. Reson. Ser. A*, **1995**, *116*, 215.

[29] a) M. J. Duer, in *Solid-State NMR Spectroscopy. Principles and Applications,* (Ed.: M. J. Duer), Blackwell Science, Oxford, **2002**, Chapter 1, pp. 3 – 72; b) U. Haeberlen, in *Advances in Magnetic Resonance*, *Supplement 1, High Resolution NMR in Solids: Selective Averaging*, (Ed. J. S. Waugh), Academic Press, New York, **1976**, pp. 1 – 190; c) C. J. Jameson, A. C. De Dios, *Nucl. Magn. Reson*. **2015**, *44*, 46, and earlier issues of this annual review; d) J. K. Harper in *Encyclopedia of NMR, Vol. 1* (Eds.: R. K. Harris, R. E. Wasylishen) Wiley, Chichester, **2012**, pp. 472 – 480.

[30] H. Nowotny, G. Heger, *Acta Crystallogr*. **1986**, *C42*, 133.

[31] O. Dmitrenko, S. Bai, P. A. Beckmann, S. van Bramer, A. J. Vega, C. Dybowski, *J. Phys. Chem. A*, **2008**, *112*, 3046.

[32] C. Dybowski, M. L. Smith, M. A. Hepp, E. J. Gaffney, G. Neue, D. L. Perry, *Appl. Spectrosc*, **1998**, *52*, 426.

[33] R. L. Sass, E. B. Brackett, T. E. Brackett, *J. Phys. Chem*, **1963**, *67*, 2863.

[34] P. Grondona, A. C. Olivieri, *Concepts Magn. Reson*, **1993**, *5*, 319.

[35] D. Massiot, I. Farnan, N. Gautier, D. Trumeau, A. Trokiner, J. P. Coutures, *Solid State Nucl. Magn. Reson.* **1995**, *4*, 241.

[36] G. M. Bernard, R. E. Wasylishen, C. I. Ratcliffe, V. Terskikh, Q. Wu, J. M. Buriak, T. Hauger, *J. Phys. Chem. A*, **2018**, *122*, 1560.

[37] Q. Xu, T. Eguchi, H. Nakayama, N. Nakamura, M. Kishita, *Z. Naturforsch.* **1991**, *46a*, 240.

[38] R. V. Pound, *Phys. Rev*. **1950**, *79*, 685.

[39] F. W. Wehrli, *Ann. Rep. NMR Spectrosc*. **1979**, *9*, 125.

[40] Benchtop NMR Blog: https://www.nanalysis.com/nmready-blog/2017/7/27/the-lightest-metal-with-a-heavyweight-demand-lithium, accessed Jan. 29, 2020.

[41] a) S. E. Ashbrook, S. Wimperis, in *Encyclopedia of NMR, Vol. 7* (Eds.: R. K. Harris, R. E. Wasylishen) Wiley, Chichester, **2012**, pp. 3675 – 3689; b) P. P. Man, in *Encyclopedia of NMR, Vol. 7* (Eds.: R. K. Harris, R. E. Wasylishen) Wiley, Chichester, **2012**, pp. 3689 – 3698.

[42] a) J. A. Pople, T. Schaefer, *Mol. Phys*. **1960**, *3*, 547, b) P. Diehl, J. A. Pople, *Mol. Phys*. **1960**, *3*, 557.

[43] Nanalysis Corp. Homepage: http://www.nanalysis.com, accessed Apr. 23, 2020.

[44] Magritek Ltd. Homepage: http://magritek.com, accessed Apr. 23, 2020.

[45] Bruker Biospin: https://www.bruker.com/products/mr/nmr/benchtop-nmr.html, accessed Apr. 23, 2020.

[46] M. K. Sørensen, O. Bakharev, O. Jensen, H. J. Jakobsen, J. Skibsted, N. Chr. Nielsen, *J. Magn. Reson*. **2014**, *238*, 20.